

Molecular dynamics evidences of the full graphitization of a nanodiamond annealed at 1500 K

J.-M. Leyssale^{a,*}, G.L. Vignoles^b

^a CNRS, Laboratoire des Composites ThermoStructuraux, UMR 5801, CNRS-Snecma Propulsion Solide-CEA-Université Bordeaux 1, 3 allée de La Boétie, Université Bordeaux 1, 33600 Pessac, France

^b Université Bordeaux 1, Laboratoire des Composites ThermoStructuraux, UMR 5801, CNRS-Snecma Propulsion Solide-CEA-Université Bordeaux 1, 3 allée de La Boétie, Université Bordeaux 1, 33600 Pessac, France

Received 8 January 2008; in final form 5 February 2008

Available online 13 February 2008

Abstract

The annealing of a small nanodiamond cluster at 1500 K is studied by molecular dynamics. The transformation of the particle in an almost fully graphitized carbon onion is observed. The remaining 17% of sp_3 atoms are delocalized on the whole particle, both under the form of isolated point defects and of small diamond-like clusters separating large graphite-like domains. It is also shown, that the Berendsen thermostat, previously used to fix temperature in such simulations, transfers kinetic energy from internal to global motions of the cluster. This can lead to severe artifacts like the freezing of the graphitization process.

© 2008 Elsevier B.V. All rights reserved.

1. Introduction

Since their discovery by Ugarte in the early 1990s [1], carbon onions or onion like carbons (OLC) have attracted a considerable amount of research. The interest for these nanoparticles, made in a first approximation of concentric graphitic shells, is motivated by their possible applications in electromagnetic devices [2], as solid lubricants [3,4] or for field emission devices [5]. Another source of interest in these particles is their possible implication as carriers of the 217.5 nm interstellar absorption bump [6]. Among the methods proposed in the literature to produce carbon onions, the high temperature annealing of ultradisperse nanodiamond clusters (NDC) [7] is probably the most popular, as it allows the production of onions with uniform size. As a consequence, the graphitization of NDCs has been extensively investigated in the past years [8–15]. It has been shown that NDC with diameters around 5 nm

transform into spherical OLC after annealing at temperatures ranging from 1373 to 2173 K [8,11,12]. The graphitization observed at 1373 K is however found to be only partial and complete transformation happens only for temperatures around 1673 K [12]. Moreover, and even when the transformation of the particle is complete, a residual sp_3 bonding signal can be detected from electron energy-loss spectroscopy, X-ray diffraction or Raman spectroscopy [8–10]. The microscopic nature of this sp_3 signal is still a question of debate. It is indeed unclear whether it is due to dangling bonds, or structural defects, connecting small sp_2 domains and delocalized in the whole particle, or to the existence of a remaining diamond domain in the core of the onions [8–10]. Molecular dynamics (MD) is a well established technique to study nanoscale transformations of matter. Very recently, Bródka et al. have published a MD investigation of the graphitization of a 3 nm spherical NDC annealed at 1200, 1500 and 1800 K [15]. At 1200 K, well below the experimental graphitization limit, they observed only a very partial graphitization of the surface of the NDC, in agreement with the bucky diamond structure observed in electronic microscopy [12]. At 1800 K, they observed the full graphitization of the particle into a

* Corresponding author.

E-mail addresses: leyssale@lcts.u-bordeaux1.fr (J.-M. Leyssale), vinhola@lcts.u-bordeaux1.fr (G.L. Vignoles).

carbon onion with a remaining 12% of tetracoordinated atoms attributed to structural defects. They also showed that the graphitization mechanism proceeds from the surface to the core of the particle as recently proposed by Qiao et al. [12]. At the intermediate temperature of 1500 K, the transformation started in the same way as at 1800 K but stopped before full graphitization. The resulting particle was composed of graphitic shells surrounding a diamond core made of around 40% of the atoms, in apparent agreement with the diamond core hypothesis mentioned earlier.

In the next section we show that the Berendsen thermostat [16] used by these authors is not adapted to the study of isolated clusters of particles and present the methodology used to re-visit this work. We then discuss our new set of results on the low temperature graphitization of a small NDC.

2. Methods

We first consider the classical molecular dynamics trajectory of N particles in an isolated cluster, obtained by solving iteratively the newtonian equations of motion $\dot{\mathbf{r}}_i = \mathbf{p}_i/m_i$ and $\dot{\mathbf{p}}_i = -\nabla_i \mathcal{U}$, where \mathbf{r}_i , \mathbf{p}_i and m_i are, respectively the position, momentum and mass of particle i , \mathcal{U} is the total potential energy and ∇_i indicates the derivative with respect to \mathbf{r}_i . These equations preserve the total energy $E = \mathcal{U} + \mathcal{K}$ (where $\mathcal{K} = \sum_{i=1}^N \mathbf{p}_i^2/m_i$ is the instantaneous kinetic energy of the system) as well as the linear momentum $\mathbf{P} = \sum_{i=1}^N \mathbf{p}_i$ and angular momentum $\mathbf{L} = \sum_{i=1}^N \mathbf{r}_i \times \mathbf{p}_i$.

As most experiments are performed at constant temperature, it is more convenient to fix temperature rather than energy in molecular dynamics simulations. From the equipartition theorem we know that each degree of freedom of the system is associated to an average kinetic energy of $k_B T/2$ from which we can define the following kinetic definition of temperature:

$$T = \frac{2}{N_f k_B} \langle \mathcal{K} \rangle \quad (1)$$

where k_B is the Boltzmann constant, N_f is the number of degrees of freedom (\mathbf{P} is usually set to zero so $N_f = 3N - 3$) and $\langle \mathcal{K} \rangle$ is the ensemble (or time) average of \mathcal{K} . The method proposed by Berendsen [16] consists in performing newtonian integration steps and then scaling the momenta after each timestep δt ($\mathbf{p}_i^{\text{new}} = \chi \mathbf{p}_i^{\text{old}}$) with the scaling factor χ defined by

$$\chi = \left[1 + \frac{\delta t}{\tau} \left(\frac{K^*}{\mathcal{K}} - 1 \right) \right]^{\frac{1}{2}} \quad (2)$$

In this equation \mathcal{K} and K^* are, respectively the actual and targeted kinetic energies ($K^* = N_f k_B T^*/2$, T^* being the targeted temperature), δt is the integration timestep and τ is the relaxation time of the thermostat ($\tau > \delta t$). With this scheme, some kinetic energy is released from (respectively given to) the system when the temperature is too high (resp. low). On average, the kinetic energy, so the temperature, is

fixed to the targeted value. The MD trajectories generated with this thermostat are not characteristic of any known statistical ensemble and this method is thus not recommended for use in molecular dynamics [17]. However, because of its simplicity, this thermostat is still used in numerous simulations studies.

It appears that this thermostat can lead to dramatic artifacts when applied to isolated clusters of particles. We know that the average kinetic energy of the system is constant under equilibrium conditions. This implies that the average heat exchanged between the system and the thermostat is null. Let us thus consider two MD integration steps for which the instantaneous kinetic energies before scaling are $\mathcal{K}_+ = K + \Delta K$ and $\mathcal{K}_- = K - \Delta K$, K being the targeted kinetic energy. The corresponding Berendsen scaling factors are $\chi_+ = \left[1 + \frac{\delta t}{\tau} \left(\frac{-\Delta K}{K + \Delta K} \right) \right]^{1/2}$ and $\chi_- = \left[1 + \frac{\delta t}{\tau} \left(\frac{\Delta K}{K - \Delta K} \right) \right]^{1/2}$. It is easy to show that the kinetic energy exchanged with the thermostat during these two steps is null ($\delta K = \delta K_+ + \delta K_- = (\chi_+^2 - 1) + (\chi_-^2 - 1) = 0$). This thermostat thus succeeds in fixing the average kinetic energy of the system. However, the effect of two such Berendsen integration steps on momenta is more problematic. The resulting linear and angular momenta are, respectively $\mathbf{P}_{+-} = \chi_+ \chi_- \mathbf{P}$ and $\mathbf{L}_{+-} = \chi_+ \chi_- \mathbf{L}$ where \mathbf{P} and \mathbf{L} are their initial values. The scaling factor $\chi_+ \chi_-$ given by Eq. (3) is always greater than 1.

$$\chi_+ \chi_- = \left[1 + \frac{\Delta K^2}{(K + \Delta K)(K - \Delta K)} \times \left(\frac{2\delta t}{\tau} - \frac{\delta t^2}{\tau^2} \right) \right]^{1/2} > 1 \quad (3)$$

Note that K and ΔK are intrinsic properties related to the temperature and heat capacity of the system and that the value of this scaling factor increases with the ratio $\delta t/\tau$, which is a property of the simulation method. The scaling of momenta induced by the use of the Berendsen thermostat is not an issue for the linear momentum, as this quantity is usually initialized at zero and so remains null. However, the use of such an algorithm implies an exponential increase of the angular momentum \mathbf{L} . The angular momentum is related to the angular velocity of the system through $\mathbf{L} = \mathbf{I}\boldsymbol{\omega}$ and the rotational kinetic energy of the system is $\mathcal{K}_{\text{rot}} = \boldsymbol{\omega} \mathbf{I} \boldsymbol{\omega}$ where \mathbf{I} is the inertia tensor of the system. We now clearly see that the Berendsen thermostat promotes an increase of the angular velocity and of the rotational kinetic energy of the system. As the system evolves at a constant average kinetic energy, the kinetic energy associated to internal motions of the system (motions of atoms with respect to the other atoms of the system) $K_{\text{int}} = K - K_{\text{rot}}$ decreases exponentially with the simulation time. Although the considerations presented here are general, we add that such a problem is not encountered when a bulk system, submitted to periodic boundary conditions, is simulated. Indeed, the rotational dynamics in such a system is violated each time a particle crosses the system boundaries, which results in a constant (null) average value for the total angular momentum of the system. However,

when an isolated cluster of particles has to be simulated, like in the present case, it is essential to use a method that conserves, at least on average, or sets to zero the angular momentum.

Similar artifacts resulting from velocity rescaling algorithms have already been reported in the literature [18,19]. Harvey et al. [18] were the first to observe such a freezing of internal degrees of freedom together with a sharp increase of global motions velocities. They explained this ‘flying ice cube’ phenomenon in terms of the transfer of kinetic energy from high frequency to low frequency vibrational modes. We show here that this artifact comes from the effect of velocity scaling on the global linear and angular momenta of the system, independently of any consideration on the vibrational frequencies of the considered motions.

In the next section we compare MD trajectories of the annealing of a nanodiamond obtained with the Berendsen thermostat to those obtained with two other well known thermostating schemes, namely the Gaussian isokinetic thermostat of Evans et al. [20] and the stochastic thermostat of Andersen [21].

Constant temperature MD using the Gaussian thermostat presents equations of motion similar to those of Newtonian dynamics, except that a friction term is added to the momenta equation $\dot{\mathbf{p}}_i = -\nabla_i \mathcal{U} - \xi \mathbf{p}_i$. The friction term ξ is a Lagrange multiplier constraining the instantaneous kinetic energy \mathcal{K} to be equal to the targeted kinetic energy K^*

$$\xi = -\frac{\sum_{i=1}^N \mathbf{p}_i \cdot \nabla_i \mathcal{U}}{\sum_{i=1}^N \mathbf{p}_i^2} \quad (4)$$

The time derivatives of the linear and angular momenta are, respectively $\dot{\mathbf{P}} = -\xi \mathbf{P}$ and $\dot{\mathbf{L}} = -\xi \mathbf{L}$ and so these quantities, if not null, are not conserved by this set of equations. We can see however from Eq. (4) that ξ is on average a positive quantity (ξ is proportional to the sum on particles of the dot product between the force acting on a particle and its momentum; this is positive on average for normal systems). As a consequence, the global momenta slowly decrease to zero during the course of a simulation. Incidentally this creates a confusion in the value of the number of degrees of freedom N_f needed to compute the temperature (Eq. (1)). If the linear momentum is initially set to zero and taking into account that one extra degree of freedom is suppressed because of the constraint of constant kinetic energy, N_f should be $3N - 4$. However, in the limit of long simulation time, this number tends towards $3N - 7$ because of the freezing of the global rotational motions. This effect is however negligible when one looks at the value of N (usually in the range 10^3 – 10^5 atoms).

In the method proposed by Andersen, the system dynamics obeys Newton’s equations but the momenta of atoms are re-drawn from a Maxwell–Boltzmann distribution at a frequency given by a Poisson law [21]. With this method, both global rotational and translational average

kinetic energies are set to $3k_B T/2$ and the temperature can be computed through Eq. (1) with $N_f = 3N$.

As in the work of Bródka et al. [15], the interactions between carbon atoms are taken into account through the reactive empirical bond order (REBO) potential of Brenner et al. [22]:

$$\mathcal{U} = \sum_i \sum_{j>i} f_c(r_{ij}) [V_R(r_{ij}) - b_{ij} V_A(r_{ij})] \quad (5)$$

where r_{ij} is the distance between carbon atoms i and j . The function $f_c(r)$ is a switching function that goes smoothly from unity for $r = 0.17$ nm to zero for $r = 0.2$ nm. $V_R(r)$ and $V_A(r)$ are, respectively the repulsive and attractive potentials and b_{ij} is an empirical bond order term taking into account the local environments of atoms i and j .

The simulated NDC of 2425 carbon atoms is a 3 nm diameter spherical chunk taken from a perfect diamond structure with initial momenta drawn from a Maxwell–Boltzmann distribution (the global linear momentum being set to zero). First order equations of motion are integrated with a Gear predictor-corrector integrator when the Gaussian thermostat is used and with a velocity-verlet integrator when Andersen or Berendsen thermostats are used [17]. In an attempt to perform a constant energy simulation of the particle with a timestep of 0.5 fs – the value adopted by Bródka et al. [15] – we observed a dramatic drift of the energy toward low values. We have thus adopted a smaller timestep, namely 0.2 fs, for which the energy conservation in absence of a thermostat is satisfactory. Simulations using the Berendsen thermostat are performed with three different values of the relaxation time τ (10, 25 and 100 fs). The value of this parameter was not reported in the paper of Bródka et al. [15]. The Andersen thermostat is set so that the momentum of an atom is re-drawn on average each 100 fs. Four MD simulations of four nanoseconds (only two nanoseconds when the Berendsen thermostat is used with a time constant of 10 fs) are performed for each thermostating method.

3. Results

We first discuss the effect of the temperature control method on the internal temperature $T_{\text{int}} = \frac{2\langle \mathcal{K}_{\text{int}} \rangle}{N_f k_B}$ and on the global rotational temperature $T_{\text{rot}} = \frac{2\langle \mathcal{K}_{\text{rot}} \rangle}{3k_B}$ in which $N_f = 3N - 6$ is the number of internal degrees of freedom, $\mathcal{K}_{\text{rot}} = \boldsymbol{\omega} \mathbf{I} \boldsymbol{\omega}$ and $\mathcal{K}_{\text{int}} = \sum_{i=1}^N \frac{p_i^2}{2m_i} - \mathcal{K}_{\text{rot}} - \mathcal{K}_{\text{trans}}$ (the global translational energy $\mathcal{K}_{\text{trans}} = \frac{P^2}{2M}$, where M is the mass of the nanoparticle, is null with both the Gaussian and Berendsen thermostat). The evolutions with time of T_{int} and T_{rot} obtained with the three thermostats are plotted in Fig. 1. Only one MD trajectory per thermostat is presented in Fig. 1 for clarity.

We can see that T_{int} is almost perfectly conserved at a value of 1500 K with the Gaussian thermostat and fluctuates around this value when the Andersen thermostat is used. Looking at the rotational temperature T_{rot} we see that it is, as expected, conserved by the Andersen thermo-

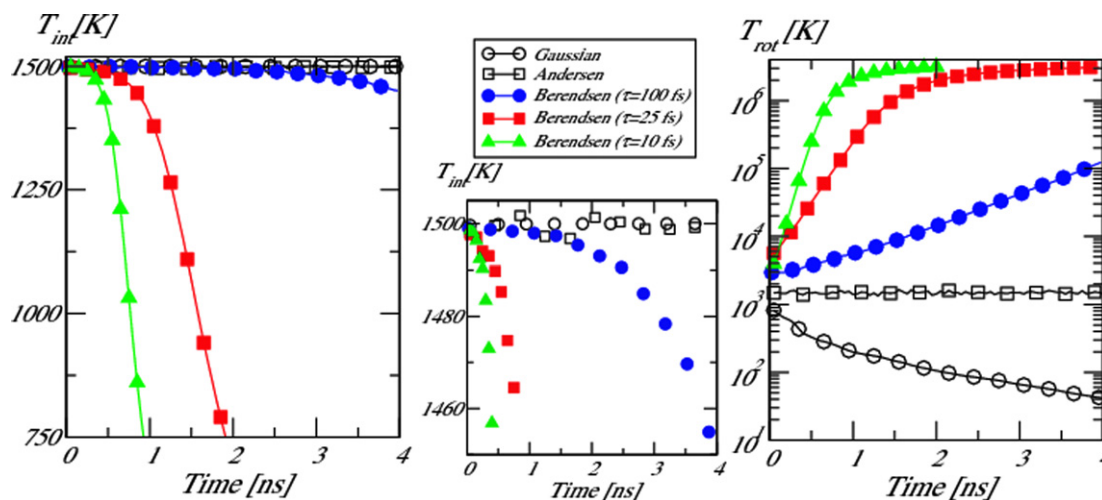


Fig. 1. Time evolution of the internal temperature T_{int} (left) and of the rotational temperature T_{rot} (right) of a 3 nm diameter spherical NDC annealed at $T = 1500$ K. Empty circles: Gaussian thermostat; empty squares: Andersen thermostat; filled symbols: Berendsen thermostat with $\tau = 100$ fs (circles), 25 fs (squares) and 10 fs (triangles). One molecular dynamics trajectory per thermostat is displayed. An enlargement on the high temperature part of the left panel is displayed on the central part of the figure, below the legend.

stat and that the Gaussian one slowly decreases it. When the Berendsen thermostat is used with a coupling constant $\tau = 100$ fs, T_{int} slowly decreases from 1500 K to 1450 K after a 4 ns MD simulation. During that time span T_{rot} is increased by almost two orders of magnitude, as can be seen in Fig. 1b. The phenomenon is the same for smaller values of the coupling constant, but is much faster. Fig. 1 shows that the lower the coupling parameter τ is, the faster the internal temperature decreases and the rotational temperature increases. When averaging on four trajectories with different initial velocities we observe after 4 ns MD trajectories an average T_{int} of 1451 K for $\tau = 100$ fs, 260 K for $\tau = 25$ fs and 216 K for $\tau = 10$ fs (after 2 ns in that case). The corresponding average rotational temperatures are, respectively 1.15×10^5 K, 3.05×10^6 K and 3.12×10^6 K. Note that the latter value is very close to the limiting case $T_{\text{rot}}^{\text{max}} = 3.6 \times 10^6$ K where all the kinetic energy ($3Nk_B T/2$) is affected to the rotation of the particle. Let us now look at the way this spurious partition of the kinetic energy affects the graphitization process.

Fig. 2 is a plot of the time evolutions of the percentage of tricoordinated (or sp_2) atoms corresponding to the five MD trajectories presented in Fig. 1. We see that when the Gaussian or the Andersen thermostat are used, the fraction of tricoordinated atoms reaches 60–70% in roughly one nanosecond. This sp_2 fraction then slowly increases towards values slightly higher than 80% at the end of the 4 ns simulations (the same average final sp_2 fraction of 82% is obtained with both the Gaussian and the Andersen thermostats). This final value is much higher than the one reported by Bródka et al. who found a plateau value of 56% [15]. It indicates that the use of these thermostats promotes an almost complete graphitization of the NDC. A similar result is obtained when the Berendsen thermostat is used with a time constant of 100 fs (average final sp_2 fraction of 82%). However, Fig. 2 shows that

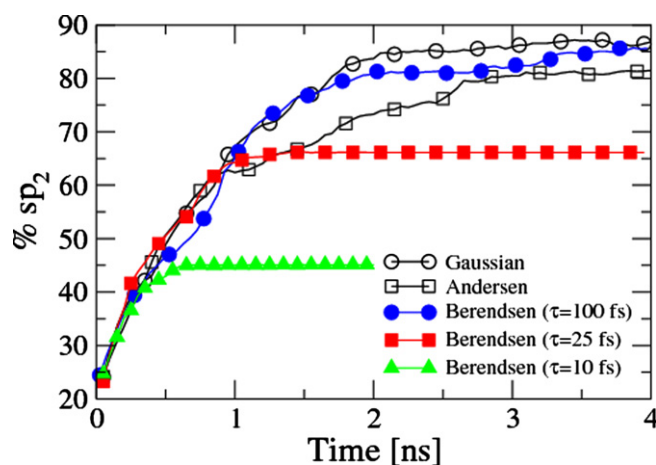


Fig. 2. Time evolution of the percentage of tricoordinated (sp_2) atoms of a 3 nm diameter spherical NDC annealed at $T = 1500$ K. Empty circles: Gaussian thermostat; empty squares: Andersen thermostat; filled symbols: Berendsen thermostat with $\tau = 100$ fs (circles), 25 fs (squares) and 10 fs (triangles). One molecular dynamics trajectory per thermostat is displayed.

the graphitization stops well earlier when this thermostat is used with smaller time constants. Indeed, we see in Fig. 2 that the graphitization stops at a sp_2 fraction of 64% (respectively 47%) after 1.5 ns (resp. 0.5 ns) of MD when a time constant of 25 fs (resp. 10 fs) is used. This is an obvious consequence of the freezing of the internal degrees of freedom observed in Fig. 1 in the same time intervals. On average, the final sp_2 fractions are 66 and 50% when time constants of, respectively 25 and 10 fs are used. This clearly shows that results obtained with the Berendsen thermostat are erroneous. We do not comment on them anymore in the remaining of this section, which deals with the graphitization mechanism and the structure of the obtained OLC. In what follows, we present the results of a single MD trajectory using the Gaussian thermostat. Other

trajectories, obtained with Gaussian, Andersen and Berendsen thermostat (with $\tau = 100$ fs) present similar features.

The mechanism of the graphitization is presented in Fig. 3. Fig. 3 a shows a slice of the NDC (0.6 nm thick) taken parallel to the $\{110\}$ diamond crystallographic plane at the beginning of the process. As can be seen in Fig. 3b, showing the same slice after 0.8 ns of MD simulation at 1500 K, the graphitization starts from the surface and progresses towards the core of the particle. We can see however that the graphitization process is not homogeneous and that at time $t = 0.8$ ns the particle is very well graphitized on both its left and right sides and remains in a diamond-like form in its core and on its top side. The process keeps on going as time goes by, as can be seen in Figs. 3c and d. Although one large diamond domain can still be observed (top-right side of Fig. 3d), the particle is almost fully graphitized at the end of the 4 ns MD simulation. Fig. 3d shows that some sp_3 atoms are also found at the boundaries between disoriented graphite-like layers and as dangling bonds between two layers. We can see however that the core of the particle is almost fully graphitized, which rules out the hypothesis of a diamond core for the particle. We show in Fig. 4 a snapshot of the final configuration of the system. Of the 2425 atoms composing the particle, only 411 (17%) are tetracoordinated. Among these

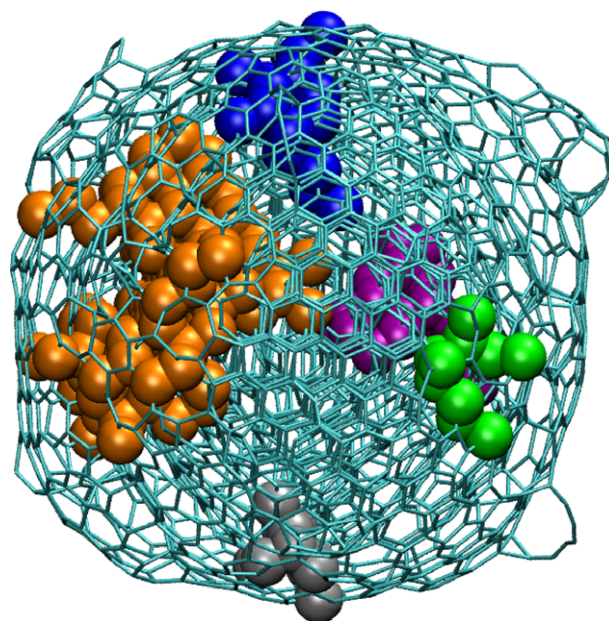


Fig. 4. Snapshot of the onion after annealing at 1500 K for 4 ns. Chemical bonds between carbon atoms are indicated by sticks (two atoms are considered bound if their distance is less than 0.18 nm). Carbon atoms belonging to sp_3 bonded clusters of at least ten atoms are displayed with coloured spheres. The clusters are composed of: 171 atoms (orange); 30 atoms (blue); 29 atoms (purple); 15 atoms (gray); 10 atoms (green) (For interpretation of the references in colour in this figure legend, the reader is referred to the web version of this article.)

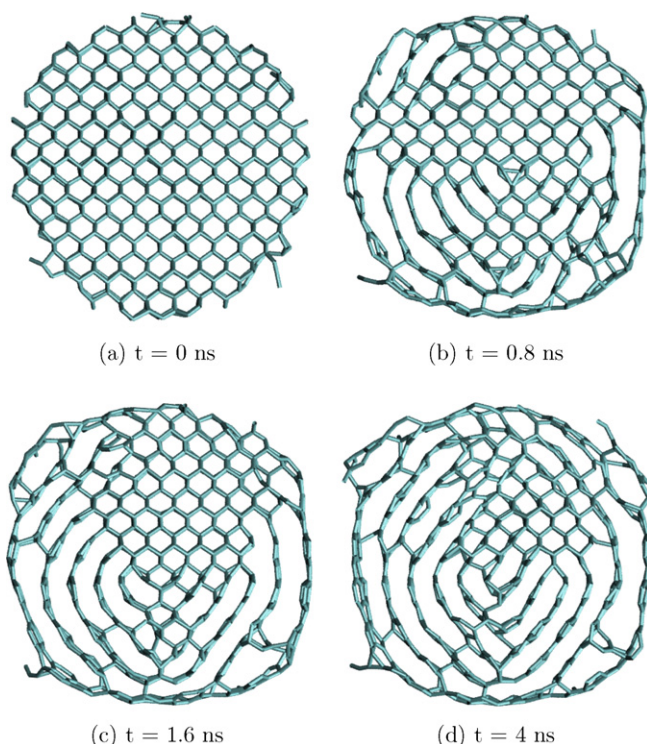


Fig. 3. 0.6 nm Thick slice of a 2425 atoms NDC annealed at 1500 K for 0 (a), 0.8 (b), 1.6 (c) and 4 (d) nanoseconds. The slice is taken to be parallel to the 110 plane of the original NDC. Bonds between carbon atoms are displayed with sticks. Two atoms are considered bound when their distance is less than 0.18 nm (a) $t = 0$ ns, (b) $t = 0.8$ ns, (c) $t = 1.6$ ns, and (d) $t = 4$ ns.

sp_3 atoms, 255 belong to clusters of at least ten atoms situated at the boundaries between graphite-like domains. More precisely, we observe one main sp_3 cluster made of 171 atoms, corresponding to the remaining sp_3 domain observed on the top-right side of Fig. 3d, and four smaller clusters made of 10–30 atoms. As can be seen in Fig. 4, these clusters appear to be randomly located in the particle. The remaining 156 sp_3 atoms belong to isolated point defects. We add that some of the MD trajectories exhibit even better graphitization properties, with no sp_3 clusters larger than 30 atoms.

4. Conclusion

Using MD simulations we have been able to show that the graphitization of a 3 nm NDC annealed at 1500 K is almost complete. The remaining 17% of sp_3 bonds are both due to the persistence of small diamond-like clusters at the boundaries between graphitization fronts and to point defects. We did not observe any diamond core in opposition to the hypothesis made by experimentalists [8–10] and to the MD results of Bródka et al. [15]. We gave evidences showing that the method used by the latter authors to control temperature is not adapted to the study of isolated systems of particles. In particular, we showed that application of the Berendsen thermostat to the annealing of NDC can lead to the freezing of the graphitization process which is exactly what these authors have observed.

Our work thus presents a new set of results on the low temperature annealing of a NDC together with a possible explanation for the residual sp_3 bonding signal observed in experiments. These results should be considered as valid for an approximative description of the system, due to the use of an empirical interaction potential. One of the main approximations of the Brenner potential, used here, is the lack of both repulsive and dispersive van der Waals interactions. It is unclear whether such an approximation can have or not a significant effect on the graphitization process; this will be a subject for future work.

Acknowledgement

We thank Dr. Jérôme Delhommelle for helpful discussions on thermostating methods. Part of the simulations have been performed at the M3PEC computing center of the Université Bordeaux 1.

References

- [1] D. Ugarte, *Nature* 359 (1992) 707.
- [2] V.L. Kuznetsov, Y.V. Butenko, A.L. Chuvilin, A.I. Romanenko, A.V. Okotrub, *Chem. Phys. Lett.* 336 (2001) 397.
- [3] A. Hirata, M. Igarashi, T. Kaito, *Tribol. Int.* 37 (2004) 899.
- [4] N. Matsumoto, L. Joly-Pottuz, H. Kinoshita, N. Ohmae, *Diamond Relat. Mater.* 16 (2007) 1227.
- [5] A.V. Okotrub, L.G. Bulusheva, A.V. Gusel'nikov, V.L. Kuznetsov, Y.V. Butenko, *Carbon* 42 (2004) 1099.
- [6] L. Henrard, P. Lambin, A.A. Lucas, *Astrophys. J.* 487 (1997) 719.
- [7] V.L. Kuznetsov, A.L. Chuvilin, Y.V. Butenko, I.Y. Mal'kov, V.M. Titov, *Chem. Phys. Lett.* 222 (1994) 343.
- [8] S. Tomita, M. Fujii, S. Hayashi, K. Yamamoto, *Chem. Phys. Lett.* 305 (1999) 225.
- [9] S. Tomita, T. Sakurai, H. Ohta, M. Fujii, S. Hayashi, *J. Chem. Phys.* 114 (2001) 7477.
- [10] S. Tomita, A. Burian, J.C. Dore, D. Le Bolloch, M. Fujii, S. Hayashi, *Carbon* 40 (2002) 1469.
- [11] J. Qian, C. Pantea, J. Huang, T.W. Zerda, Y. Zhao, *Carbon* 42 (2004) 2691.
- [12] Z. Qiao, J. Li, N. Zhao, C. Shi, P. Nash, *Scr. Mater.* 54 (2006) 225.
- [13] V.Y. Osipov et al., *Carbon* 44 (2006) 1225.
- [14] Z. Qiao, J. Li, N. Zhao, C. Shi, P. Nash, *Chem. Phys. Lett.* 429 (2006) 479.
- [15] A. Bródka, T.W. Zerda, A. Burian, *Diamond Relat. Mater.* 15 (2006) 1818.
- [16] H.J.C. Berendsen, J.P.M. Postma, W.F. van Gunsteren, A. Di Nola, J.R. Haak, *J. Chem. Phys.* 81 (1984) 3684.
- [17] M.P. Allen, D.J. Tildesley, *Computer Simulation of Liquids*, Oxford University Press, Oxford, 1987.
- [18] S.C. Harvey, R.K.-Z. Tan, T.E. Cheatman III, *J. Comput. Chem.* 19 (1998) 726.
- [19] S.-W. Chiu, M. Clark, S. Subramaniam, E. Jakobsson, *J. Comput. Chem.* 21 (2000) 121.
- [20] D.J. Evans, G.P. Morriss, *Statistical Mechanics of Nonequilibrium Liquids*, Academic Press, London, 1990.
- [21] H.C. Andersen, *J. Chem. Phys.* 72 (1980) 2384.
- [22] D.W. Brenner, O.A. Shenderova, J.A. Harrison, S.J. Stuart, B. Ni, S.B. Sinnott, *J. Phys. Condens. Matter* 14 (2002) 783.